University of Tehran Press

Online ISSN: 2345-475X

DESERT

Home page: https://jdesert.ut.ac.ir/

Derivation and Functional Evaluation of Pedotransfer Functions for Estimating the Soil Water Infiltration Rate

Rahman Barideh[1*], Fereshteh Nasimi[2], Alireza Tavasolee[1], Ahmad Bybordi[1], Reza Hassanpour[1], Yaser Hamdi Ahmadabad[3]

[1] Agricultural Research, Education and Extension Organization (AREEO), East Azerbaijan, Tabriz, Iran Email: r.barideh@areeo.ac.ir
[2] Department of Water Sciences, Urmia University, West Azerbaijan, Urmia, Iran
[3] Agricultural Research, Education and Extension Organization (AREEO), West Azerbaijan, Urmia, Iran

Article Info.

Article type:
Research Article

Article history:
Received: 24 Jan. 2026
Received in revised from: 03 Mar. 2026
Accepted: 03 Apr. 2026
Published online: 09 Apr. 2026

Keywords:
Error function,
Double ring,
Multiple linear regression,
Recalibration.

ABSTRACT

Direct measurement of soil water infiltration can be laborious, time-consuming, and expensive under certain conditions. The main objective of this study was to investigate the possibility of accurately estimating the final soil water infiltration rate (IR) using pedotransfer functions (PTFs) based on readily available soil attributes (RASAs). In this study, new PTFs were derived from a small regional dataset, and the performance of existing PTFs was evaluated in comparison with the locally developed ones. Furthermore, an approach was proposed to improve IR estimation by developing error functions based on basic soil properties and adding the predicted error to the estimated IR values. In addition, a recalibration approach was applied to enhance the performance of existing PTFs at the local scale. To this end, IR, soil texture, bulk density, organic matter, geometric mean diameter, geometric standard deviation of particle size, specific surface area, and structural stability index were measured in two adjacent regions (T1 and T2). The IR data were obtained using the double-ring method at 49 points in T1 and 27 points in T2, with three replications. Using the T1 dataset, PTFs were developed through multiple linear regression (MLR), and both new and existing PTFs were validated using the T2 dataset. . The results showed that none of the considered PTFs could accurately estimate IR (34%<nRMSE<5678%) but the use of error functions (25%<nRMSE<104%) and recalibration of the existing PTFs (18%<nRMSE<30%) considerably increased the accuracy of the IR estimations. Consequently, even with a limited number of data (N=15), one can develop error functions or recalibrate the existing PTFs to improve their estimation accuracy in practice.

Cite this article: Barideh, R., Nasimi, F., Tavasolee, A.R., Baybordi, A., Hassanpour, R., Hamdi, Y. (2026). Derivation and functional evaluation of pedotransfer functions for estimating the soil water infiltration rate. DESERT, 31 (1), DOI: 10.22059/jdesert.2026.107375

DOI: 10.22059/jdesert.2026.107375

Publisher: University of Tehran Press

1. Introduction

Given the world's growing population, there is an urgent need for water to improve food and fiber production. On the other hand, available water resources have been severely reduced for several reasons including an improper use in various sectors. Consequently, in the recent decades, many efforts have been made to invent new irrigation methods for effective water use. To this end, it is vital to pay attention to the soil water infiltration rate, which serves a significant role in the effective management of water resources, as well as in designing and planning all irrigation methods. Furthermore, infiltration plays an important role in the hydrological cycle influencing runoff and soil erosion, solute transport and groundwater pollution thus determining vegetation diversity and, more in general, the region's ecology (Pahlavan-Rad *et al*., 2020; Mirzaee *et al*., 2014; Rashidi *et al*., 2014; Parchami-Araghi *et al*., 2013).

Hillel (1982) defined infiltration as "the process of water entry into the soil, generally by downward flow through all or part of the soil surface". Factors affecting soil water infiltration rate (IR) include texture (Brady and Weil, 1996) and structure of soil (Brady and Weil, 1996; Lin *et al*., 1999), bulk density (Assouline, 2006), soil compaction (Hillel, 1982) and soil porosity (Ehlers, 1975; Hillel, 1982; Šimůnek *et al*., 2003), initial soil water content and vegetation type (Ehlers, 1975), soil surface slope (Lal and Shukla, 2004; Hatt and LeCoustumer, 2008), precipitation rate and soil trapped air (Wangemann *et al*., 2000), type of clay minerals (Ben-Hur and Assouline, 2002), and various land management factors (Moroke *et al*., 2009).

Historically, several models have been proposed for the mathematical description of IR (Green and Ampt, 1911; Richards, 1931; Kostiakov, 1932; Horton, 1941; Philip, 1957; Holtan, 1961; Smith, 1972; Soil Conservation Service, 1972; Brutsaert, 1977; Haverkamp *et al*., 1994; Parlange *et al*., 2002), which need measured data points to be parameterized. However, since the direct measurement of soil water infiltration is laborious, time-consuming and expensive at least in certain circumstances, some indirect methods such as pedotransfer functions (PTFs) have been suggested to estimate IR based on readily available soil attributes (RASAs). The term PTF was coined by Bouma (1989) as translating data we have into what we need. The most readily available data comes from a soil survey, such as the field morphology, soil texture and structure. PTFs add value to this basic information by translating them into estimates of other more laborious and expensively determined soil properties. Actually, PTFs are mathematical equations that estimate difficult to measure soil parameters (e.g., IR) using readily available or easily measurable soil parameters, such as soil texture and bulk density. While there are numerous approaches to derive these PTFs, multiple linear regression (MLR) is the most common one as it is convenient and simple to use; also, the results can be easily interpreted (Sepahvand *et al*., 2021; Moraes *et al*., 2020; Lee *et al*., 2019; Kumar and Sihang, 2019; Sepahvand *et al*., 2019; Zhang *et al*., 2017).

So far, numerous PTFs have been derived, even recently, to estimate IR based on soil physical and environmental properties (Pahlavan-Rad *et al*., 2020; Sepahvand *et al*., 2021; Rashidi *et al*., 2014; Pandey and Pandey, 2018; Patle *et al*., 2019). The persisting interest for this kind of PTFs has practical explanations. For example, these tools could be used in remote areas, where direct measurement of IR is hampered by problems related to the availability of time and water for direct testing. As most of these PTFs are applicable only in specific agro-pedo-climatic conditions, their use is often restricted to the specific geographic area and/or the particular soil type for which they were derived. The reliability of PTFs applied in a region different from the one for which they were originally derived is often limited as a result of the differences in geologic, geohydrologic, climatic and land use factors (Weynants *et al*., 2009).

So, their extrapolation potential is still in question and, in any case, it is expected to generally be limited. In other terms, it is still necessary to verify if there are means to improve prediction of IR without making workloads practically unaffordable.

Therefore, the main objective of this study was to investigate the possibility of accurately estimating the soil water infiltration rate (IR) using PTFs based on readily available soil attributes (RASAs) outside their derivation regions. Specifically, we derived some new PTFs based on a small regional dataset and tested the estimation reliability of existing PTFs in contrast to the predictions made by our PTFs. Furthermore, we tested the possibility to improve the soil IR estimations by correcting the estimated values of IR with a "prediction error" that was estimated from specifically developed PTFs. In this study, we have also proposed an approach to use the existing PTFs for local to regional-scale applications by recalibrating the existing PTFs to improve the estimation of the soil IR at the local scales.

2. Materials and methods

2.1. Study area

The present study was carried out in the Khoda-Afarin region, in the north of East-Azerbaijan Province, northwest Iran. Measurements were performed at two different but adjacent sites (T1 and T2) with a distance of 15 km from each other. The T1 and T2 sites were selected from agricultural lands with an area of 125 and 82 hectares, respectively (Figure 1). The region had a mean annual rainfall and temperature of 354 mm and 13.8°C, respectively. The regional climate was a moderate semi-arid and semi-arid one based on Embereger and De-Martonn methods, respectively.

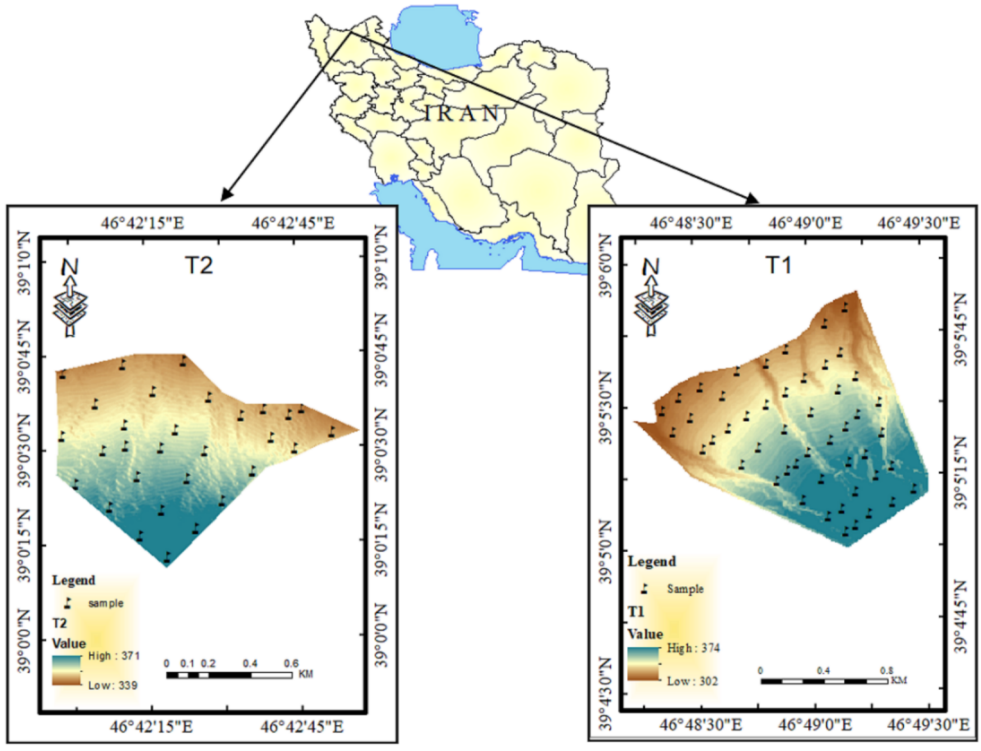

Figure 1. Map of the study area and sampling locations in T1 and T2 sites

2.2. Field measurements

The IR data were obtained using the double-rings method with outer and inner ring diameters of 60 and 30 cm for 49 points in T1 and 27 points in T2 sites. Measurements at every point were replicated in three. The distance between replicates was about 2.5 m with a triangular pattern (Ghorbani-Dashtaki *et al*., 2016) (Figure 2). For this purpose, the existing plants were removed with a knife without damaging the soil surface before ring insertion. At the beginning of the experiment, a thin sheet of plastic was used inside the rings to avoid the surface soil disturbance due to the splashing action of the poured water (Pandey and Pandey, 2018). Then the rings were filled with water to a height of 10 cm and when the water level inside the rings reached about 3 cm, they were refilled simultaneously to a height of 10 cm. The choice to characterize a sampling site by three replicated measurements of IR was made since infiltration is highly variable even at very short spatial scales and a near-point in the field could be better characterized by averaging a few closely spaced replicated measurements rather than by a single measurement (Gonzalez-Sosa *et al*., 2010; Bagarello *et al*., 2019). Water infiltration into the soil was continued until a steady state condition was observed (USDA-NRCS, 2005). Initial volumetric soil water content, θ_i (cm^3cm^{-3}), and bulk density, ρ_b ($g\ cm^{-3}$), were estimated by using the cylinder method and oven-drying (Grossman and Reinsch, 2002; Punamia *et al*., 2005); soil particle size distribution was determined by the hydrometer method (Gee and Or, 2002) and the soils were classified by the USDA textural classification system (Figure 3); regarding the organic matter, OM (%), the Walkley and Black method (Walkley and Black, 1934) was applied.

2.3. Calculated parameters

The soil particle size distribution, bulk density and organic carbon are not sufficient inputs to characterize the pore structure of soils (Pachepsky *et al*., 2006) and, hence they could not be enough to predict IR by a PTF (Ghorbani-Dashtaki *et al*., 2016). However, less is known about the possibility to conveniently organize the basic information in the perspective to improve prediction of IR. Therefore, different additional parameters were considered in this investigation. In particular, the geometric mean, dg (mm), and the geometric standard deviation, σg, of the soil particle diameter were obtained by using the method proposed by Shirazi and Boersma (1984) (eqs. 1-2); the soil specific surface area, SSA ($g\ m^{-2}$) was obtained using the method developed by Sepaskhah and Tafteh (2013) (eq. 3); further, soil structural stability index, SSI (%) was obtained by using Pieri's (1992) method (eq. 4).

$$d_g = e^a;\ a = 0.01 \sum_{i=1}^{n} F_i \ln(M_i) \quad (1)$$

$$\sigma_g = e^b;\ b^2 = 0.01 \sum_{i=1}^{n} F_i \ln^2(M_i) - a^2 \quad (2)$$

$$SSA = e^{(10.66 \times D - 25.06)};\ D = 3 - 0.118\left[\left(\frac{Si+Sa}{100}\right) - Ln\left(\frac{Cl}{100}\right)\right] \quad (3)$$

$$SSI = \left(\frac{OC \times 1.724}{Cl+Si}\right) \times 100 \quad (4)$$

where n=3 is the number of soil separate groups (e.g., sand, silt and clay), Fi is the percentage of the total soil mass, ln is the natural logarithm, Mi is the arithmetic mean of two consecutive particles-size limits, Cl is the percentage of clay, Si is the percentage of silt, Sa is the percentage of sand, D is the fractal dimension of the pore–solid interface and OC is the soil organic carbon. SSI > 9% indicates a stable structure, 7% < SSI ≤ 9% suggests a low risk of structural degradation, 5% < SSI ≤ 7% reflects a high risk of degradation, and SSI ≤ 5% refers to a

structurally degraded soil (Reynolds *et al*., 2009; Pieri, 1992).

Figure 2. Triangular pattern of replicated field double-rings runs and the corresponding soil sampling location

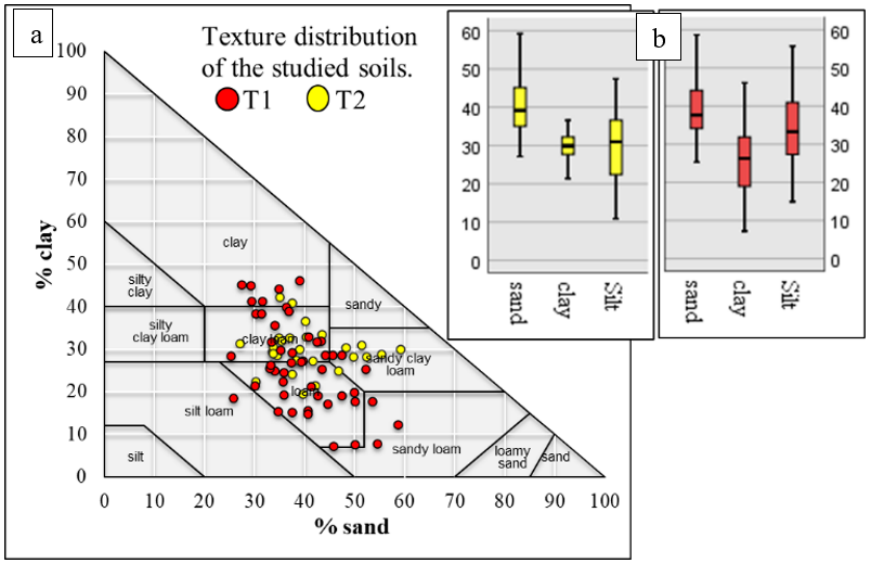

Figure 3. Textural distribution of the studied soils in T1 and T2 sites (a), and the box plots of sand, silt and clay contents (b)

2.4. Derivation and evaluation of PTFs

To derive new PTFs for estimating infiltration rate (EIR), the correlation matrix was obtained by the Pearson correlation test, while the Shapiro-Wilk and Kolmogorov-Smirnov tests were used to test the normality of data. Then, PTFs were derived using the MLR and the best selection method in the SPSS software (v.26). PTFs were derived using 85% of the T1 data that were randomly selected; their validity was evaluated using the remaining data. Furthermore, the T2 data were used to evaluate the reliability of PTFs in the estimation of IR for the data set other than the one used to derive them, i.e., outside their derivation site.

2.5. Selected PTFs for examination

In this study, we examined the accuracy and reliability of four different existing PTFs presented by Rashidi *et al*. (2014), Pandey and Pandey (2018), and Patle *et al*. (2019) to estimate the final infiltration rate (EIR) outside their derivation regions. The accuracy of PTFs was examined using the T2 data. PTFs are reported in Table 1.

Table 1. The original forms of the pedotransfer functions selected for the estimation of IR

PTFs	Reference	PTF name
EIR = -30578.81-305.56×Sa-306.16×Si-306.33×Cl-15.18×ρb+4.18×ρs+0.34×θv +16.85×OC	Patle *et al*. (2019)	Patle PTF
EIR = -144.64+1.65×Sa-1.57×Si-0.42×Cl-1.79×ρb+1.22×ρs-0.11×θv+0.66×OC	Pandey and Pandey (2018)	Pandey PTF
EIR = 0.391×Sa - 2.917	Rashidi *et al*. (2014)	Rashidi PTF1
EIR = 28.13-0.220×Si-0.5182×Cl+4.592×ρb-1.440×OM+0.022×θv	Rashidi *et al*. (2014)	Rashidi PTF2

EIR (cm h^{-1}): estimated infiltration rate, Sa (%): sand, Si (%): silt, Cl (%): clay, ρb (g cm^{-3}): bulk density, ρs (g cm^{-3}): particle density, θv (cm^3 cm^{-3}): volumetric moisture, OC (%): organic carbon, OM (%): organic matter

2.6. PTFs Recalibration

The purpose of this step was to determine the minimum data required to recalibrate PTFs outside their derivation regions to improve the estimation of IR. Therefore, the coefficients of the independent variables of PTFs were recalculated using 20%, 30%, 40%, 50%, 60% and 70% of the datasets; at each step, their validity was evaluated using the remaining data. At each step, the datasets were randomly selected. These steps were performed for T1 and T2 datasets, separately.

2.7. Error functions

This step was intended to develop the error functions (EF) to improve the PTFs performance. So, it was assumed that the difference between the measured and PTFs-estimated values of IR (Measured – PTFs-estimated = Error) depended on RASAs. Therefore, to improve the performance of PTFs outside their derivation region, the error function was added to the original PTFs (new PTFs = original PTFs + error functions). The error functions were derived using 50% of the T2 dataset and MLR method in the SPSS software (v.26). The accuracy of the new PTFs was evaluated using the remaining data.

2.8. Statistical analysis

The following statistical indices were used to evaluate the performance of the derived PTFs.

$$R^2 = 1 - \frac{\sum_{i=1}^{n}(O_i - P_i)^2}{\sum_{i=1}^{n}(O_i - \overline{O})^2} \quad (5)$$

$$RMSE = \sqrt{\frac{\sum_{i=1}^{n}(O_i - P_i)^2}{n}} \quad (6)$$

$$nRMSE = \frac{RMSE}{\overline{O}} \quad (7)$$

$$AE = \frac{100}{n}\sum_{i=1}^{n}\frac{|O_i - P_i|}{O_i} \quad (8)$$

$$GMER = \exp\left[\frac{1}{n}\sum_{i=1}^{n}\ln\left(\frac{Pi}{O_i}\right)\right] \quad (9)$$

where n is the number of data, Oi and Pi are the measured and predicted data values, and ō is the mean of the measured data values. The coefficient of determination [R^2 (-)] is a measure of the linear association between the measured and PTFs-estimated values. The range of R^2 changes from 0 to 1; the values close to unity indicated the better performance of PTFs (Tashayo *et al*., 2020). The root mean square error [RMSE (cm h^{-1})] represents the difference between the estimated and actual value; it is always positive. For a good model performance, the values of RMSE should be close to 0 (Barideh & Nasimi, 2024, 2025). Normalized root mean square error [nRMSE (%)] indicates the relative difference of the estimated versus measured data. The estimation is considered excellent if nRMSE≤10%, good if 10%<nRMSE≤20%, fair if 20%<nRMSE≤30%, and poor if nRMSE>30% (Andarzian *et al*., 2011; Nasimi *et al*., 2025). Absolute relative error [AE (%)] is used for the reliable estimation; values closer to 0 show the good performance of the model (Pahlavan-Rad *et al*., 2020). When the value of the geometric mean error ratio [GMER (-)] is less or greater than unity, it indicates underestimation or overestimation of the model, respectively (Abdelbaki, 2016).

3. Results and discussion

3.1. Soil attributes

Table 2 presents the descriptive statistics of RASAs and IR in T1 and T2 sites. The mean measured IR in T1 was 4.8 cm h^{-1}, ranging from 2.2 to 7 cm h^{-1}. Based on the value of the first and third quarters (3.1 and 6.3%), the mean value (4.9%) and the range of SSI (0.3 to 9.9%), 50% of the soil structure was degraded, 20% was at a high risk of degradation, and 30% was at a low risk of degradation. In T2, the IR ranged from 2.2 to 5.6 cm h^{-1} with the mean 3.9 cm h^{-1}. Based on the SSI range from 1.77 to 7.58%, with the first and third quarters, which were 3.38 and 5.17%, respectively, with the mean value of 4.47%, 75% of the soil structure was degraded; also, 25% was at a high risk of degradation.

Table 2. Descriptive statistics related to the measured readily available soil attributes (RASAs) and infiltration rates in T1 and T2

	T1						
	Min	Max	Mean	1st quartile	3rd quartile	Standard deviation	Coefficient of variation
Sa (%)	25.30	58.70	39.30	33.80	44.40	7.80	19.80
Si (%)	14.90	55.70	34.30	27.20	41.20	8.70	25.40
Cl (%)	7.20	46.10	26.40	18.70	32.40	10.20	38.50
ϕ (-)	0.40	0.50	0.40	0.43	0.47	0.02	5.50
ρb (g cm^{-3})	1.34	1.58	1.46	1.40	1.51	0.06	4.41
θv (-)	0.17	0.33	0.25	0.23	0.29	0.04	14.18
OM (%)	0.42	4.72	2.65	1.87	3.35	0.95	35.73
dg (mm)	0.02	0.15	0.05	0.03	0.07	0.03	58.87
σg (-)	9.04	24.19	15.63	12.92	18.55	3.45	22.05
SSA (m^2 g^{-1})	11.49	193.99	82.40	44.05	104.74	48.75	59.16
SSI (%)	0.30	9.90	4.92	3.11	6.32	2.26	45.89
IR (cm h^{-1})	2.20	7.00	4.80	4.10	5.70	1.20	24.40

Table 2. Continued

	T2						
	Min	Max	Mean	1st quartile	3rd quartile	Standard deviation	Coefficient of variation
Sa (%)	27.10	59.20	40.70	34.90	46.80	7.70	19.00
Si (%)	10.90	47.40	29.50	22.10	36.90	8.80	29.70
Cl (%)	19.50	42.20	29.80	27.30	31.80	5.10	16.90
ϕ (-)	0.37	0.50	0.45	0.42	0.48	0.03	7.40
ρb (g cm^{-3})	1.31	1.67	1.46	1.38	1.53	0.09	6.04
θv (-)	0.19	0.32	0.25	0.22	0.28	0.04	14.58
OM (%)	1.16	4.40	2.59	1.86	2.98	0.81	30.68
dg (mm)	0.02	0.09	0.05	0.03	0.06	0.02	35.26
σg (-)	12.31	22.62	17.87	15.68	20.63	2.84	15.58
SSA (m^2 g^{-1})	46.95	165.60	93.06	79.20	101.57	26.63	28.08
SSI (%)	1.77	7.58	4.47	3.38	5.17	1.56	34.21
IR (cm h^{-1})	2.20	5.60	3.90	3.00	4.60	1.00	25.30

IR: infiltration rate, Sa: sand, Si: silt, Cl: clay, ϕ: Porosity, ρb: bulk density, θv: volumetric moisture, OM: organic matter, dg: geometric mean of the soil particle diameter, σg: geometric standard deviation of the soil particle diameter, SSA: soil-specific surface area and SSI: structural stability index

3.2. Correlation between IR and soil attributes

The correlations between the measured IR and RASAs are displayed in Table 3. Since the T2 data was used to evaluate PTFs outside their derivation regions and PTFs were derived from the T1 data, the correlation matrix was only investigated for these data. IR had a positive relationship with Si, Cl, OM, σg and SSA, and a negative relationship with Sa, ρb, θv, dg and SSI. The highest correlation was observed between IR and sand content. Similar results have been obtained by other researchers. For example, Patle *et al*. (2019) and Rashidi *et al*. (2014) reported that the sand content had a great influence on IR; also, Pandey and Pandey (2018) showed that the correlation between IR and sand was 0.88. Therefore, in this study, two PTFs were derived. The first PTF was derived by using the sand content as the input, since the soil textural data is the most available data and the sand content had the highest correlation to IR in our study (Table 3), while the second one was got by applying other parameters.

Table 3. Correlation matrix of the measured soil attributes in T1

	Sa	Si	Cl	ρb	θv	OM	dg	σg	SSA	SSI	IR
Sa	1										
Si	-0.24	1									
Cl	-0.56**	-0.67**	1								
ρb	0.75**	-0.11	-0.48**	1							
θv	0.59**	-0.14	-0.33**	0.43**	1						
OM	-0.31*	0.17	0.09	-0.10	-0.09	1					
dg	0.85**	0.20	-0.82**	0.64**	0.51**	-0.31*	1				
σg	-0.15	-0.89**	0.87**	-0.14	-0.09	0.05	-0.60**	1			
SSA	-0.53**	-0.68**	0.99**	-0.47**	-0.30*	0.06	-0.77**	0.84**	1		
SSI	0.70**	-0.40*	-0.19	0.39**	0.44**	-0.21	0.49**	0.12	-0.18	1	
IR	-0.66**	0.15	0.38*	-0.38*	-0.42**	0.36*	-0.63**	0.17	0.36*	-0.38**	1

** Significant at 1% probability level, * Significant at 5% probability level, IR: infiltration rate, Sa: sand, Si: silt, Cl: clay, ϕ: Porosity, ρb: bulk density, θv: volumetric moisture, OM: organic matter, dg: geometric mean of the soil particle diameter, σg: geometric standard deviation of the soil particle diameter, SSA: soil-specific surface area and SSI: structural stability index

3.3. Derivation and evaluation of PTFs

Table 4 shows the derived PTFs for IR. The first PTF was derived by using the sand content; meanwhile, the second PTF was obtained using ρb, Cl, dg and SSA. PTFs were formed using 85% of the T1 data which were selected randomly and their interpolation accuracy was evaluated using the remaining data (Figure 4). R^2 and RMSE were 0.41 and 0.94 cm h^{-1} for PTF1; these were 0.47 and 0.85 cm h^{-1} for PTF2. The fitting was considered good in both PTFs according to the value of nRMSE (19.42% and 17.56%). In the evaluation step, at their derivation regions, the accuracy of PTF1 with the value of RMSE=0.48cm h^{-1}, nRMSE=10% and GMER=0.99 was higher than that of PTF2 (Table 5).

Table 4. Derived PTFs used to EIR

EIR=8.724-0.099×Sa	PTF1
EIR=6.858+3.81×ρb-0.31×Cl-58.51×dg+0.046×SSA	PTF2

EIR: estimated infiltration rate

Table 5. Validation indices of derived PTFs used to EIR

	Fitting in T1				
	R^2(-)	RMSE(cm h^{-1})	nRMSE(%)	AE(%)	GMER(-)
PTF1	0.41	0.94	19.42	17.51	1.03
PTF2	0.47	0.85	17.56	15.84	0.98
	Validation in T1				
	R^2(-)	RMSE(cm h^{-1})	nRMSE(%)	AE(%)	GMER(-)
PTF1	0.68	0.48	10.01	8.36	0.99
PTF2	0.80	0.52	11.05	7.81	1.04

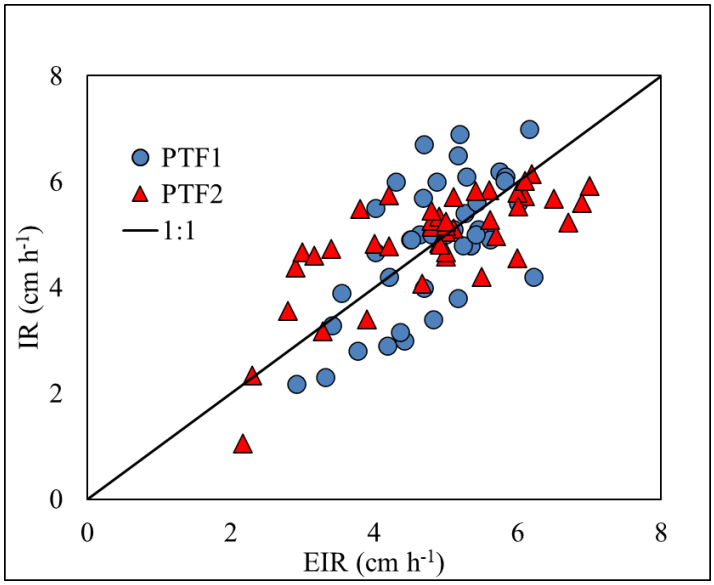

Figure 4. Observed versus estimated values of IR using PTF1 and PTF2 in Fitting step

3.4. Evaluation of PTFs outside their derivation regions

In this study, we investigated the accuracy and performance of six different PTFs (Tables 1 and 4) outside their derivation regions. Table 5 and 6 also show the accuracy of the examined PTFs in their derivation regions. According to the values of R^2, RMSE and nRMSE, the accuracy of PTFs was in a good range.

Table 6. The accuracy of the investigated PTFs in their derivation regions

	Rashidi PTF1	Rashidi PTF2	Pandey PTF	Patle PTF
R^2(-)	0.89	0.908	0.92	0.89
RMSE(cm h^{-1})	2.55	2.320	0.38	1.10
nRMSE(%)	25.00	22.780	5.90	23.10

Table 7 and Figure 5 show the results of estimating IR in T1 and T2. It was revealed that none of PTFs could estimate infiltration rate (EIR) with an appropriate accuracy. The highest value of R^2 was related to Rashidi PTF2, with the value of 0.098; the nRMSE value of all PTFs was higher than 30% (indicating poor predictive performance). Hence, it could be concluded that it was not practically advisable to use such PTFs outside their derivation regions and they could not be used without recalibration.

The inefficiency of PTFs outside their derivation regions could be interpreted by examining the correlation between IR and soil properties at each equation derivation site (Table 8). Since the correlation between IR and soil properties differed in each location, the independent variables coefficients of PTFs are site-specific yielding a bias in prediction when PTFs are applied outside the calibration region. Therefore, to use PTFs outside their derivation regions, two methods including develop error functions and recalibration were investigated.

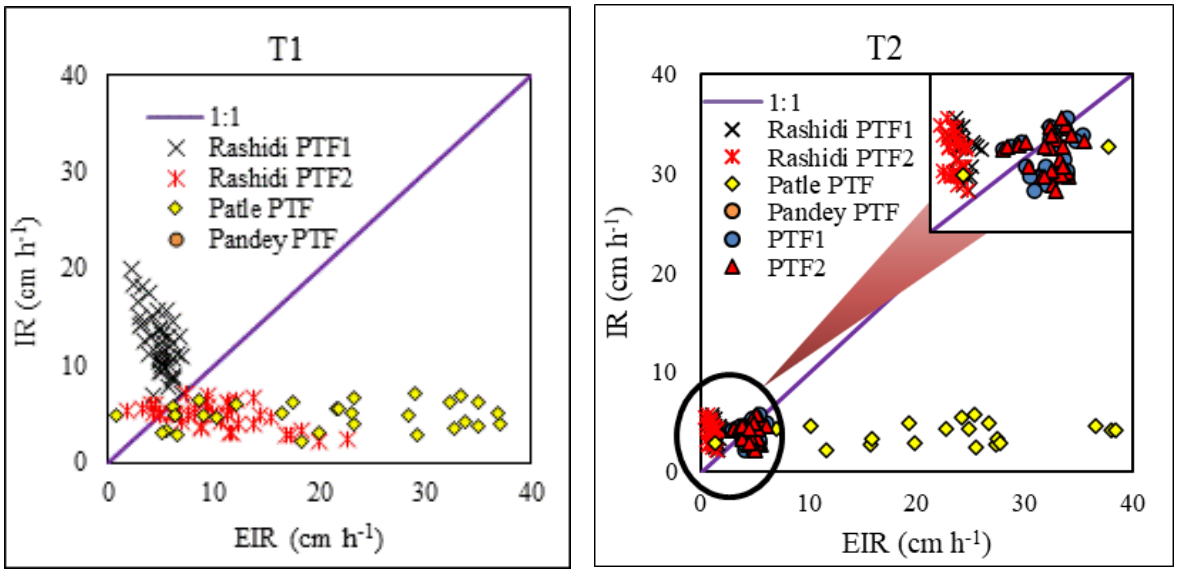

Figure 5. Observed versus predicted values of the investigated PTFs outside their derivation regions

Table 7. Statistical indices for the investigated PTFs in T1 and T2

	PTF 1	PTF 2	Patle PTF		Pandey PTF		Rashidi PTF1		Rashidi PTF2	
	T2	T2	T1	T2	T1	T2	T1	T2	T1	T2
R^2 (-)	0.00	0.00	0.00	0.00	0.00	0.00	0.03	0.02	0.09	0.09
RMSE (cm h^{-1})	1.37	1.51	24.301	23.48	216.53	224.18	2.35	2.86	3.09	3.18
nRMSE (%)	34.70	38.40	598.60	594.80	5753.20	5678.90	69.30	72.50	78.10	80.60
AE(%)	35.60	39.10	542.40	525.10	6102.70	5992.30	59.40	64.30	70.60	72.80

Table 8. Correlation between IR and soil measured attributes in their study regions

	sand	silt	clay	ρb	θv	OM
IR(Pandey)	0.88	-0.57	-0.78	-0.74	-0.67	0.34
IR(Patle)	0.75	-0.41	-0.73	-0.33	-0.22	0.22
IR(Rashidi)	0.94	-0.85	-0.86	0.80	-0.48	-0.69
IR(T1)	-0.66	0.15	0.38	-0.38	-0.42	0.36
IR(T2)	-0.16	0.01	0.23	-0.39	-0.20	0.11

3.5. Recalibration of PTFs

In order to determine the minimum data required to recalibrate PTFs outside their derivation regions to improve the estimation of IR, the independent variables coefficients of PTFs were recalibrated using 20%, 30%, 40%, 50%, 60% and 70% of the datasets; at each step, their accuracy was evaluated using the remaining data. We recalibrated all the PTFs and reevaluated them. Since there was no considerable difference among the PTFs in terms of their reliability as affected by recalibration, we only presented the results for PTFs 1 and 2. Figure 6 shows RMSE, nRMSE and AE for each dataset and the number of measurements per hectare. The accuracy of PTFs showed a positive nonlinear increase with raising the number of data; so, with data greater than 40% in T1 and 50% in T2, inconsiderable changes were observed. Consequently, in this study, by using one measurement for every six hectares, PTFs could be recalibrated to reach an acceptable accuracy equal to that in their derivation step. Also, Taulya *et al*. (2005), in a recalibration study of soil bulk density PTFs, concluded that the recalibration of PTFs reduced the model's bias and improved its precision.

3.6. Error functions

Table 9 shows the error functions and variations of RMSE and nRMSE for the investigated PTFs in T2 between the initial prediction and the modified one by adding the error function (EF). Error functions were derived using 50% of the T2 data; then they were added to PTFs; the accuracy of the modified predictions (EIR+EF) was evaluated using the remaining data. In general, RMSE and nRMSE values showed that the use of error functions increased the accuracy of the PTFs prediction, making it possible to use them outside their derivation regions. The lowest and highest values of RMSE were related to Rashidi PTF1 and Patle PTF, respectively. It is noteworthy that the nRMSE value of the Pandey PTF was 5548%; after adding the ER, this value was decreased to 27%,

becoming one of the most accurate PTFs. Figure 7 shows the measured IR versus the modified prediction using the ER. Shaker *et al*. (2019), testing new inputs to predict the near-saturated soil hydraulic conductivity, used the error function, concluding that the use of error functions increased the accuracy of the PTFs prediction.

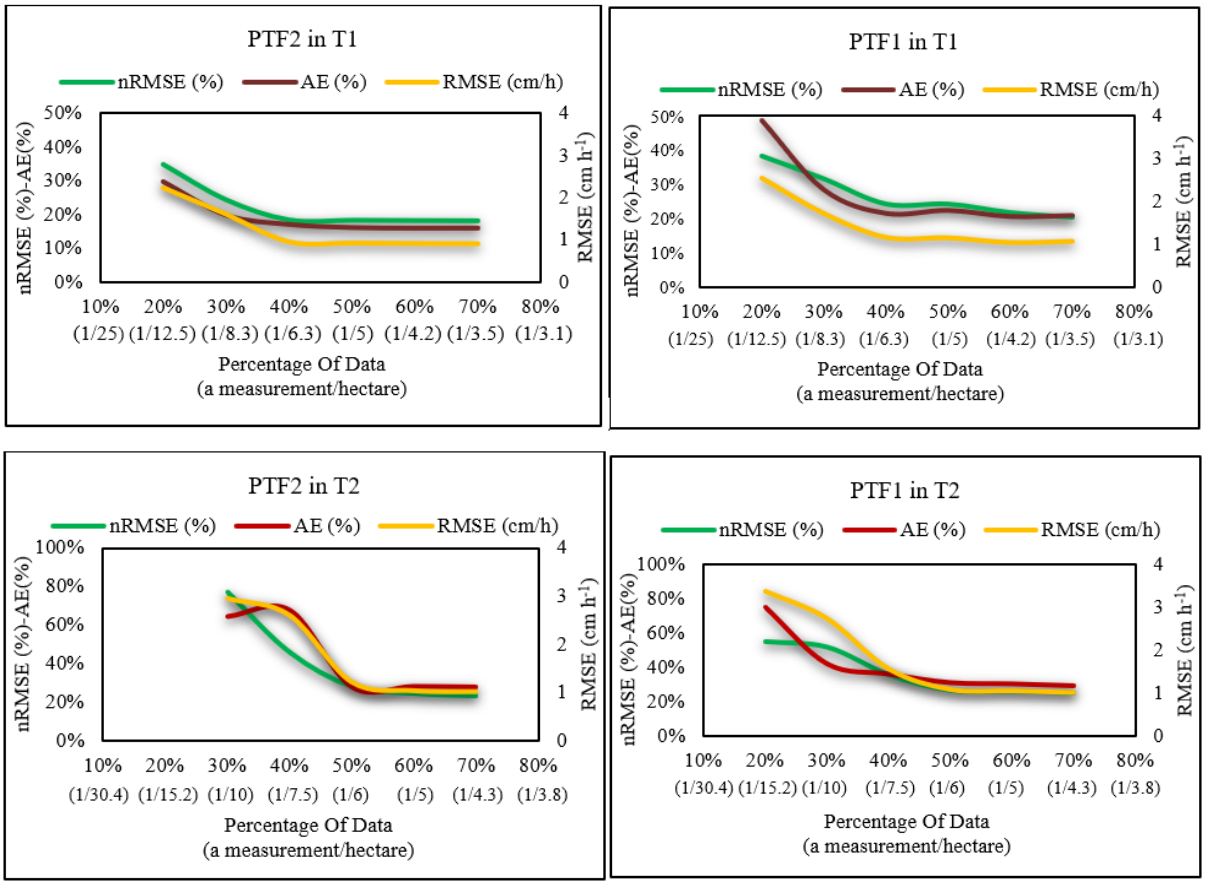

Figure 6. Recalibration of the infiltration rate of PTF1 and PTF2 in T1 and T2

Table 9. The values of statistical indices for the investigated PTFs in T2 through coupling the pedotransfer function and EF

PTF name	Error function	RMSE (cm h^{-1})		nRMSE (%)	
		EIR	EIR+EF	EIR	EIR+EF
PTF1	EF =1.59-0.08×Si	1.3	1.1	32	27
PTF2	EF =1.258-0.085×Si+0.12×ρb	1.5	1.2	38	30
Patle PTF	EF =317.8-3.72×Sa-3.05×Si-18×OM-0.5×SSA	24.9	4.2	616	104
Pandey PTF	EF =400.7-4.31×Sa-1.43×OM	224	1.1	5548	27
Rashidi PTF1	EF =4.8-0.05×Sa	2.9	1.0	73	25
Rashidi PTF2	EF =0.59+0.11×Cl	3.2	1.2	80	30

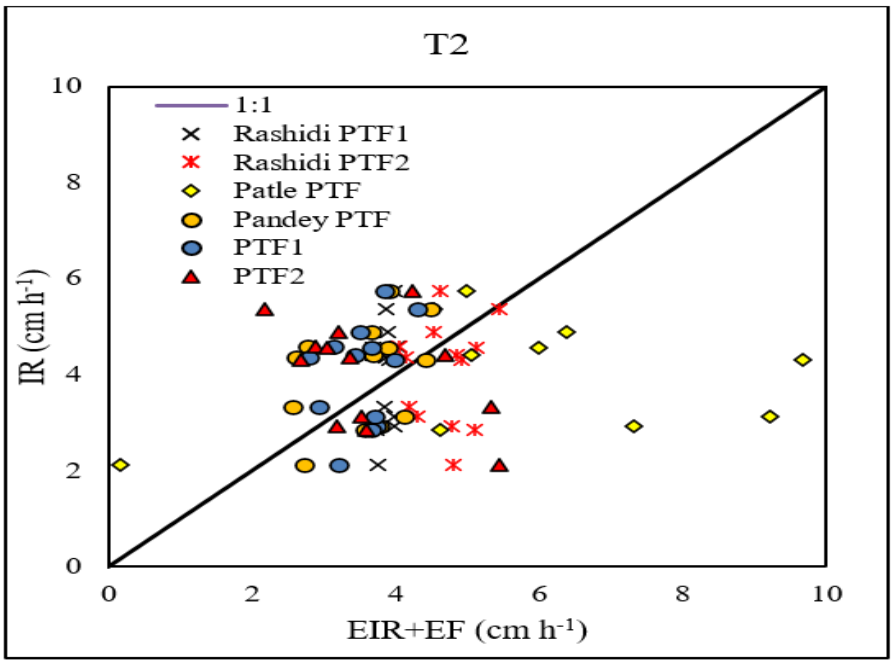

Figure 7. Measured versus the modified estimation IR by adding EF

4. Conclusions

This study investigated the possibility of estimating the soil water infiltration rate (IR) using pedotransfer functions (PTFs) based on readily available soil attributes (RASAs), the accuracy of extrapolation of derived PTFs, and the minimum data required to recalibrate PTFs and develop error functions to improve their performance. Measurements were conducted in two different regions (T1 and T2). Using the T1 dataset and multiple linear regression (MLR), PTFs were developed and then validated using the T2 dataset.

In the fitting step, two PTFs were derived. The first PTF was based on sand content, while the second one was developed using bulk density (ρb), clay content (Cl), geometric mean diameter (dg), and specific surface area (SSA). The fitting performance of both PTFs was acceptable according to statistical indices, indicating that they can be used with reasonable accuracy within their derivation region.

However, the extrapolation results showed that none of the PTFs could estimate IR with acceptable accuracy outside their derivation region, as all nRMSE values exceeded 30%. Therefore, the direct application of these PTFs without calibration is not recommended. To address this limitation, two approaches—development of error functions and recalibration—were evaluated.

The results indicated that the accuracy of PTFs in the recalibration step increased nonlinearly with increasing data volume. When more than 40% of the data in T1 and 50% in T2 were used, further improvements became negligible. In addition, the use of error functions improved the prediction accuracy of PTFs. These findings demonstrate that even with a limited dataset (N = 15), it is possible to enhance the performance of existing PTFs through recalibration or error function development. Overall, recalibration is recommended for simpler PTFs, while the use of error functions can be considered for more complex PTFs that are difficult to calibrate.

Acknowledgments
The authors would like to thank all participants of the present study.

Authors Contribution
Conceptualization, R.B., F.N.; methodology, R.B., F.N., A.T.; software, R.B., F.N.; validation, R.B., F.N., A.B., R.H.; formal analysis, R.B.; investigation, R.B., F.N., A.T., Y.H.A.; resources, R.B., F.N., A.T., A.B., Y.H.A.; data curation, R.B., F.N., A.T.; writing—original draft preparation, R.B.; writing—review and editing, R.B., F.N.; visualization, R.B.; supervision, R.B.; project administration, R.B., F.N.; funding acquisition, R.B. All authors have read and agreed to the published version of the manuscript.

Ethics approval and Consent to participate
The authors avoided from data fabrication and falsification.

Competing Interests
The authors declare no conflicts of interest.

Funding
This research did not receive any specific grant from funding agencies in the public, commercial, or not-for-profit sectors.

Consent for Publication
Not applicable.

Data Availability
The authors confirm that the data supporting the findings of this study are available within the article [and/or] its supplementary materials.

References

Abdelbaki, A.M. (2016). Using automatic calibration method for optimizing the performance of Pedotransfer functions of saturated hydraulic conductivity. *Ain Shams Engineering Journal, 7*(2), 653-662. https://doi.org/10.1016/j.asej.2015.05.012

Andarzian, B., Bannayan, M., Steduto, P., Mazraeh, H., Barati, M., Barati, M., & Rahnama, A. (2011). Validation and testing of the AquaCrop model under full and deficit irrigated wheat production in Iran. *Agricultural Water Management, 100*, 1–8. https://doi:10.1016/j.agwat.2011.08.023

Assouline, S. (2006). Modeling the relationship between soil bulk density and the hydraulic conductivity function. *Vadose Zone Journal, 5*(2), 697-705. https://doi.org/10.2136/vzj2005.0084

Barideh, R., & Nasimi, F. (2024). GEE RET: Cloud-based reference evapotranspiration calculation with google earth engine. *Theoretical and Applied Climatology, 155*(9), 8887–8895. https://doi.org/10.1007/S00704-024-05152-W/METRICS

Barideh, R., & Nasimi, F. (2025). A novel approach to estimating drought-Induced damage in rainfed wheat cultivation using modified drought indices. *Theoretical and Applied Climatology, 156*(10), 1–15. https://doi.org/10.1007/S00704-025-05772-W

Ben-Hur, M., & Assouline, S. (2002). Tillage effects on water and salt distribution in a Vertisol during effluent irrigation and rainfall. *Agronomy Journal, 94*(6), 1295-1304. https://doi.org/10.2134/agronj2002.1295

Bouma, J. (1989). Using soil survey data for quantitative land evaluation. *Advances in Soil Science, 9*, 177–213.

Brady, N.C., & Weil, R.R., (1996). *The nature and properties of soils*. Prentice-Hall Inc.

Brutsaert, W. (1977). Vertical infiltration in dry soils. *Water Resources Researc,.13*, 363–368.

Ehlers, W. (1975). observations on earthworm channels and infiltration on tilled and untilled loess soil. *Soil Science, 119*(3), 242-249. https://dx.doi.org/10.1097/00010694197503000-00010

Gee, G.W., & Or, D. (2002). Particle-size analysis: Methods of soil analysis. *Madison*, 255–293.

Ghorbani-Dashtaki, G.H., Homaee, M., & Loiskandl, W. (2016). Towards using pedotransfer functions for estimating infiltration parameters. *Hydrological Sciences Journal, 61*(8), 1477-1488. https://doi.org/10.1080/02626667.2015.1031763

Green, W.H., & Ampt, G.A. (1911). Studies on soil physics. *Journal of Agricultural Science, 4*(1), 1–24. https://doi.org/10.1017/S0021859600001441

Grossman, R.B., & Reinsch, T.G. (2002). Bulk density and linear extensibility. In: Dane, J.H., Topp, G.C. (Eds.), Methods of Soil Analysis. Part 4. SSSA Book Series No. 5. Soil Science Society of America, Madison, WI.

Hatt, B., & Le-Coustumer, S. (2008). *PRACTICE NOTE 1: In Situ Measurement of Hydraulic Conductivity*. Facility for Advancing Water Biofiltration.

Haverkamp, R., Ross, P.J., Smettem, K.R.J., & Parlange, J.Y. (1994). Three dimensional analysis of infiltration from discinfiltrometer: 2. Physically-based infiltration equation. *Water Resources Research, 30*, 2931–2935.

Hillel, D. (1982). *Introduction to soil physics*. Academic press, New York.

Holtan, H.N. (1961). *A concept for infiltration estimates in watershed engineering*. USDA Agricultural Research Service. Publication ARS.

Horton, R.E. (1941). An approach toward a physical interpretation of infiltration-capacity. *Soil Science Society of America Journal, 5*, 399–417. https://doi.org/10.2136/sssaj1941.036159950005000C0075x

Kostiakov, A.N. (1932). On the dynamics of the coefficient of water percolation in soils and on the necessity for studying it from a dynamic point of view for purposes of amelioration. *Trans, 6*, 17–21.

Kumar, M., & Sihang, P. (2019). Assessment of infiltration rate of soil using empirical and machine learning-based models. *Irrigation and Drainage, 68*, 599–601. https://doi.org/10.1002/ird.2332

Lal, R., & Shukla, M.K. (2004). *Principles of soil physics*. CRC Press.

Lee, Y., Jung, G., & Kim, S. (2019). Spatial distribution of soil moisture estimates using a multiple linear regression model and Korean geostationary satellite (COMS) data. *Agriculture Water Manage, 213*, 580–593. https://doi:10.1016/j.agwat.2018.09.004

Lin, H., McInnes, K., Wilding, L., & Hallmark, C. (1999). Effects of soil morphology on hydraulic properties II. Hydraulic pedotransfer functions. *Soil Science Society of America Journal, 63*(4), 955-961. https://doi.org/10.2136/sssaj1999.634955x

Mirzaee, S., Zolfaghari, A.A., Gorji, M., Dyck, M., & Ghorbani-Dashtaki, S. (2014). Evaluation of infiltration models with different numbers of fitting parameters in different soil texture classes. *Archives of Agronomy and Soil Science, 60*(5), 681–693. https://doi.org/10.1080/03650340.2013.823477

Moraes, A.G.L., Carvalho, D.F., Antunes, M.A.H., Ceddia, M.B., & Flanagan, D.C. (2020). Steady infiltration rate spatial modelling from remote sensing data and terrain attributes in southeast Brazil. *Geoderma, 20*, e00242. https://dx.doi.org/10.1016/j.geodrs.2019.e00242

Moroke, T., Dikinya, O., & Patrick, C. (2009). Comparative assessment of water infiltration of soils under different tillage systems in eastern Botswana. *Physics and Chemistry of the Earth, 34*(4), 316-323. https://doi:10.1016/j.pce.2008.08.002

Nasimi, F., Barideh, R., & Baybordi, A. (2025). Satellite-based monitoring of water productivity of irrigated wheat in Urmia Lake basin using RUE and SEBAL algorithms and Landsat 8 and 9 images. *Agricultural Water Management, 319*, 109784. https://doi.org/10.1016/J.AGWAT.2025.109784

Pachepsky, Y.A., Rawls, W.J., & Lin, H.S. (2006). Hydropedology and pedotransfer functions. *Geoderma, 131*, 308–316. https://doi.org/10.1016/j.geoderma.2005.03.012

Pahlavan-Rad, M., Dahmardeh, K.H., Hadizadeh, M., Keykha, K.H., Mohammadni, N., Gangali, M., Keikha, M., Davatgar, N., & Brungard, C. (2020). Prediction of soil water infiltration using multiple linear regression and random forest in a dry flood plain, eastern Iran. *Catena, 194*, 104715. https://doi.org/10.1016/j.catena.2020.104715

Pandey, P.K., & Pandey, V. (2018). Estimation of infiltration rate from readily available soil properties (RASPs) in fallow cultivated land. *Sustainable Water Resources Management, 2*. https://doi.org/10.1007/s40899-018-0268-y

Parchami-Araghi, F., Mirlatifi, S.M., Dashtaki, G.S., & Mahdian, M.H. (2013). Point estimation of soil water infiltration process using artificial neural networks for some calcareous soils. *Journal of Hydrology, 481*, 35–47. https://doi:10.1016/j.jhydrol.2012.12.007

Parlange, J.Y., Barry, D.A., & Haverkamp, R. (2002). Explicit infiltration equations and the Lambert W-function. *Advances in Water Resources, 25*(8–12), 1119– 1124.

Patle, G.H., Sikar, T.T., Singh, R.K., Sudhir, K.S. (2019). Estimation of infiltration rate from soil properties using regression model for cultivated land. *Geology, Ecology, and Landscapes, 3*(1). https://doi.org/10.1080/24749508.2018.1481633

Philip, J.R. (1957). The theory of infiltration: the infiltration equation and its solution. *Soil Science, 83*, 345–358. https://doi.org/10.1097/00010694-200606001-00009

Pieri, C.J. (1992). *Fertility of Soils: A Future for Farming in the West African Savannah*. Springer-Verlag. Berlin, Germany.

Punamia, B.C., Jain, A.K., & Jain, A.K. (2005). Soil mechanics and foundations. Proceedings of the 16th thoroughly revised and enlarged edition; Dec 15; Laxmi Pub.House; New Delhi. p. 8170087910. ISBN: 9788170087915.

Rashidi, M., Ahmadbeyki, A., & Hajiaghaei, A. (2014). Prediction of soil infiltration rate based on some physical properties of soil. *American-Eurasian Journal of Agricultural and Environmental Science, 14*(12), 1359–1367. https://doi:10.5829/idosi.aejaes.2014.14.12.12461

Reynolds, W.D., Drury, C.F., Tan, C.S., Fox, C.A., & Yang, X.M. (2009). Use of indicators and pore volume-function characteristics to quantify soil physical quality. *Geoderma, 152*(3), 252-263. https://doi:10.1016/j.geoderma.2009.06.009

Richards, L.A. (1931). Capillary conduction of liquids through porous mediums. *Journal of Applied Physics, 1*, 318–333. https://doi.org/10.1063/1.1745010

Sepahvand, A., Singh, B., Ghobadi, M., & Sihag, P. (2021). Estimation of infiltration rate using data-driven models. *Arabian Journal of Geosciences, 14*, 42. https://doi.org/10.1007/s12517-020-06245-2

Sepahvand, A., Singh, B., Sihag, P., Nazari, A., Ahmadi, H., & FizNia, S. (2019). Assessment of the various soft computing techniques to predict sodium absorption ratio (SAR). *Journal of Hydraulic Engineering.* 1-12. https://doi.org/10.1080/09715010.2019.1595185

Sepaskhah, A., & Tafteh, A. (2013). Pedotransfer function for estimation of soil-specific surface area using soil fractal dimension of improved particle-size distribution. *Archives of Agronomy and Soil Science, 59*(1). https://doi:10.1080/03650340.2011.602632

Shaker, P., Khodaverdilo, H., & Momtaz, H. (2019). Testing of new inputs to predict near-saturated soil hydraulic conductivity. *Applied Soil Research, 7*(1), 54-69.

Shirazi, M.A., & Boersma, L. (1984). A unifying quantitative analysis of soil texture. *Soil Science Society of America Journal, 48*, 142–147. https://doi.org/10.2136/sssaj1984.03615995004800010026x

Šimůnek, J., Jarvis, N.J., VanGenuchten, M.T., & Gärdenäs, A. (2003). Review and comparison of models for describing non-equilibrium and preferential flow and transport in the vadose zone. *Journal of Hydrology, 272*(1), 14-35. https://doi.org/10.1016/S0022-1694(02)00252-4

Smith, R.E. (1972). The infiltration envelope: results from a theoretical infiltrometer. *Journal of Hydrology, 17*(1–2), 1–22. https://doi.org/10.1016/0022-1694(72)90063-7

Soil Conservation Service. (1972). *National engineering handbook: Hydrology*. Department of Agriculture. Washington DC. 762.

Tashayo, B., Honarbakhsh, A., Akbari, M., & Ostovari, Y. (2020). Digital mapping of Philip model parameters for prediction of water infiltration at the watershed scale in a semi-arid region of Iran. *Geoderma Regional, 22*. https://doi.org/10.1016/j.geodrs.2020.e00301

Tauya, G., Tenywa, M.M., Majaliwa, M.J.G., Odong, T.L., Kaingo, J., & Kakone, A. (2005). Validation of pedotransfer functions for soil bulk density estimation on a Lake Victoria Basin soilscape. *African Crop Science Conference Proceedings, 7*, 1049-1056.

US Department of Agriculture Natural Resources and Conservation Service (NRCS). (2005). *National Engineering Handbook: Surface Irrigation*. National Technical Information Service. Washington DC. 623.

Walkley, A., & Black, I.A. (1934). An examination of Degtjareff method for determining soil organic matter and proposed modification of the chromic acid titration method. *Soil Science, 37*, 29-37. https://doi:10.1097/00010694-193401000-00003

Wangemann, S., Kohl, R., & Molumeli, P. (2000). Infiltration and percolation influenced by antecedent soil water content and air entrapment. *American Society of Agricultural and Biological Engineers, 43*, 1517-1523. https://doi:10.13031/2013.3051

Weynants, M., Vereecken, H., & Javaux, M. (2009). Revisiting Vereecken pedotransfer functions: introducing a closed-form hydraulic model. *Vadose Zone Journal, 8*, 86-95. https://doi:10.2136/vzj2008.0062

Zhang, H., Wu, P.A., Yin, A., Yang, X., Zhang, M., & Gao, C. (2017). Prediction of soil organic carbon in an intensively managed reclamation zone of eastern China: A comparison of multiple linear regressions and the random forest model. *Science of The Total Environment, 592*, 704–713. https://doi.org/10.1016/j.scitotenv.2017.02.146